

1 **Characterizing the body morphology of the first metacarpal in the Homininae**
2 **using 3D geometric morphometrics**

3

4 Jonathan Morley¹, Ana Bucchi^{2,3}, Carlos Lorenzo^{2,3}, Thomas A. Püschel^{4*}

5

6 ¹Department of Zoology, University of Oxford, South Parks Road, OX1 3PS, Oxford,
7 United Kingdom.

8 ²Àrea de Prehistòria, Universitat Rovira i Virgili (URV), Avinguda de Catalunya 35,
9 43002 Tarragona, Spain.

10 ³Institut Català de Paleoecologia Humana i Evolució Social (IPHES), Zona
11 Educacional 4, Campus Sescelades URV (Edifici W3), 43007 Tarragona, Spain.

12 ⁴Primate Models for Behavioural Evolution Lab, Institute of Cognitive and Evolutionary
13 Anthropology, School of Anthropology, University of Oxford, 64 Banbury Road, OX2
14 6PN, Oxford, United Kingdom.

15

16 *Corresponding author:

17 Thomas A. Püschel

18 E-mail: thomas.puschelrouliez@anthro.ox.ac.uk

19 Phone: +44 (0) 7476608464

20

21 Running title: Characterizing MC1's morphology in the Homininae

22

23

24

25

26 **Abstract**

27 Objectives: Extinct hominins can provide key insights into the development of tool use,
28 with the morphological characteristics of the thumb of particular interest due to its
29 fundamental role in enhanced manipulation. This study quantifies the shape of the first
30 metacarpal's body in the extant Homininae and some fossil hominins to provide
31 insights about the possible anatomical correlates of manipulative capabilities.

32 Materials and methods: The extant sample includes MC1s of modern humans (n=42),
33 gorillas (n=27) and chimpanzees (n=30), whilst the fossil sample included *Homo*
34 *neanderthalensis*, *Homo naledi* and *Australopithecus sediba*. 3D geometric
35 morphometrics were used to characterize the overall shape of MC1's body.

36 Results: Humans differ significantly from extant great apes when comparing overall
37 shape. *H. neanderthalensis* mostly falls within the modern human range of variation
38 although also showing a more robust morphology. *H. naledi* varies from modern
39 human slightly, whereas *A. sediba* varies from humans to an even greater extent.
40 When classified using a linear discriminant analysis, the three fossils are categorized
41 within the *Homo* group.

42 Discussion: The results are in general agreement with previous studies on the
43 morphology of the MC1. This study found that the modern human MC1 is
44 characterized by a distinct suite of traits, not present to the same extent in the great
45 apes, that are consistent with an ability to use forceful precision grip. This morphology
46 was also found to align very closely with that of *H. neanderthalensis*. *H. naledi* shows
47 a number of human-like adaptations consistent with an ability to employ enhanced
48 manipulation, whilst *A. sediba* apparently presents a mix of both derived and more
49 primitive traits.

50 **Keywords:** MC1; 3D geometric morphometrics; Semi-landmarks; Hominins; African
51 apes

52

53 **1 Introduction**

54 There is no doubt that the extremely dexterous human hand is unmatched among
55 animals. As a result, the human hand has been the subject of considerable
56 paleoanthropological research over the years in order to provide a better
57 understanding of the processes that led to its evolution (Almécija, Smaers, & Jungers,
58 2015a; Key, 2016; Lewis, 1977; Marzke & Marzke, 2000; Susman, 1998). Much of
59 this has been directed at how the hand morphology of higher primates correlates to
60 their manipulative capabilities, and how fossil morphology can be used to infer tool
61 use in extinct hominin species (Almécija & Alba, 2014; Kivell, Kibii, Churchill, Schmid,
62 & Berger, 2011; Marchi, Proctor, Huston, Nicholas, & Fischer, 2017; Napier, 1955).
63 The thumb and its components, most notably the first metacarpal (MC1), plays a
64 fundamental role in object manipulation and the study of its anatomy has therefore
65 been at the center of research in this field (Galletta, Stephens, Bardo, Kivell, & Marchi,
66 2019; Marchi et al., 2017). However, the constant discovery of new fossils (e.g. *Homo*
67 *Naledi*; Berger et al., 2015) and the development of new morpho-functional analysis
68 tools mean that there is still much about the tool use behaviors and manipulative
69 capabilities of extinct hominins that is yet to be uncovered.

70 Amongst the extant great apes, humans possess the superior manipulative
71 capabilities, with the ability not only to adeptly utilize the objects in their environment,
72 but also to manufacture complex tools in ways that require high levels of dexterity.
73 These advanced skills are facilitated in part by a unique thumb morphology: the human
74 thumb is long relative to the length of the fingers compared to other less dexterous

75 apes, with powerful thenar musculature and robust thumb bones (Almécija, Moyà-
76 Solà, & Alba, 2010; Almécija et al., 2015; Feix, Kivell, Pouydebat, & Dollar, 2015;
77 Tuttle, 1969).

78 In comparison to human hands, non-human great apes, especially chimpanzees and
79 orangutans, have longer, robust fingers relative to their shorter, more gracile thumbs,
80 which is probably the result of selective pressures associated with locomotor
81 behaviors such as suspension and knuckle-walking (Almécija et al., 2015; Püschel,
82 Marcé-Nogué, Chamberlain, Yoxall, & Sellers, 2020; Richmond & Strait, 2000). Both
83 gorillas and chimpanzees have been observed using tools in the wild, to varying
84 degrees; however, their manipulative capabilities are limited due to the constraints
85 imposed by their hand morphology. Chimpanzees are prolific tool users, known to use
86 tools both in nature and captivity (Boesch & Boesch, 1990). Examples of chimp tool
87 use include termite fishing with specially crafted sticks (Sanz, Call, & Morgan, 2009),
88 hunting bush babies with sharp spears and nut-cracking with stones (Sanz & Morgan,
89 2007). Gorillas are less reliant on tool use due the fact that they exploit food resources
90 differently from chimpanzees (e.g., crack nuts with their teeth), but they have been
91 observed using sticks to test the depth of water and to support themselves when
92 crossing deep water (Breuer, Ndoundou-Hockemba, & Fishlock, 2005). However,
93 whilst non-human great apes do regularly use their thumbs to manipulate objects, they
94 are not as efficient as humans in using forceful precision grips (Marzke, Marchant,
95 McGrew, & Reece, 2015; Marzke & Wullstein, 1996).

96 Traditionally it was believed that extinct hominin species also fell into this category,
97 lacking the manual dexterity of modern humans (Lewis, 1977; Niewoehner, 2001,
98 2006; Rightmire, 1972). However, there is a growing body of evidence that many

99 hominins as early as *O. tugenensis* (Gommery & Senut, 2006) show the capacity to
100 efficiently use tools, with the ability to use forceful precision grips as dexterously as
101 humans (Alba, Moyà-Solà, & Köhler, 2003; Feix et al., 2015; Karakostis, Hotz, Scherf,
102 Wahl, & Harvati, 2017; Kivell et al., 2011; Tocheri, Orr, Jacofsky, & Marzke, 2008).
103 Human-like features would have been present along with traits suitable for arboreal
104 locomotion, which lead to the suggestion that the hominin hand evolved in a mosaic
105 fashion showing a manual morphology adapted to these two functional demands (i.e.,
106 manipulation and locomotion) (Kivell et al., 2011; Kivell, 2015). This mixed morphology
107 is apparent in the hand of *A. sediba* and *H. naledi* (Kivell et al., 2011; 2015) whereas
108 the hand of Neanderthals would be fully derived (Tocheri et al., 2008).
109 Several studies have focused on different anatomical features of the hand in an effort
110 to understand the extent to which the hand of early hominins is adapted to
111 manipulative abilities (e.g., Almécija et al., 2010; Galletta et al., 2019; Green & Gordon,
112 2008; Skinner et al., 2015), in particular regarding the joint areas of the MC1, as this
113 bone plays a crucial role in complex manipulative behaviors. However, whilst there is
114 now a greater understanding of the manipulative capabilities of hominins, much of the
115 research on the MC1 dates back to the past century and often contained only
116 qualitative assessments (Aubriot & Tubiana, 1981; Barmakian, 1992; Imaeda, An, &
117 Cooney, 1992; Napier, 1956, 1960; Tuttle, 1969). Even the most recent quantitative
118 research that has been conducted using three-dimensional geometric morphometric
119 (3DGM) techniques have focused only on those certain areas of the MC1 deemed to
120 be most important in controlling manipulation, such as the trapeziometacarpal joint
121 connecting the thumb to the wrist (i.e., proximal articular surface; Marchi et al., 2017)
122 and the first metacarpal distal articular surface (Galletta et al., 2019). As a result, most
123 of MC1's morphology (i.e., its body) has yet to be fully quantitatively analyzed to

124 assess its possible importance when assessing possible correlates with manipulative
125 abilities.

126

127 Consequently, in this study body morphology of the MC1 was quantified using 3DGM
128 in order help in the identification of structures in extant species that may be correlated
129 with human-like manipulative capabilities and determining if similar morphologies are
130 present in fossil hominins. The sample investigated in this study included three extant
131 African ape genera (*Homo*, *Gorilla*, *Pan*) and three fossil hominins (*Homo*
132 *neanderthalensis*, *Homo naledi* and *Australopithecus sediba*). Based on previous
133 literature about thumb morphology and function, the following hypotheses were tested:

134 **Hypothesis 1: MC1 morphology significantly differs between humans and extant**
135 **great ape species**

136 Though great apes use their hand for manipulative activities, their specialisation is
137 more a consequence of their locomotion (i.e., knuckle-walking and arborealism)
138 (Almécija, Moyà-Solà, & Alba, 2010). It is therefore expected that the selective
139 pressures associated with locomotor behaviour in chimpanzees and gorillas will result
140 in an MC1 morphology that varies significantly from that of bipedal humans.
141 Furthermore, different use of the human thumb during manipulation and human
142 adaptations to precise and forceful tool use are expected to lead to an MC1
143 morphology that differs from other extant apes.

144 **Hypothesis 2: All fossil hominin specimens exhibit an MC1 morphology more**
145 **similar to humans than other great apes**

146 *H. neanderthalensis*, *A. sediba* and *H. naledi* have overall hand morphologies that
147 appear to align with human hands to a greater extent than those of non-human great

148 apes. They possess adaptations, such a long thumb and short fingers, that are
149 associated with advanced manipulative capabilities in modern humans (Holliday et al.,
150 2018; Kivell et al., 2011). Given these morphological characteristics and the inferred
151 tool using abilities of *H. naledi*, *A. sediba* and *H. neanderthalensis* in previous studies,
152 they would be expected to have an MC1 morphology more closely aligned with
153 humans than gorillas or chimpanzees.

154 **2 Material and methods**

155 **2.1 Sample**

156 The extant sample used in this study includes MC1s of modern humans (*Homo*
157 *sapiens*; n=42), chimpanzees (*Pan troglodytes*; n=30), and gorillas (*Gorilla gorilla* and
158 *Gorilla beringei*; n=27) (Table S1). The human MC1s came from a medieval cemetery
159 in Burgos, Spain (Casillas Garcia & Alvarez, 2005) and the surface models were
160 obtained using a Breuckmann SmartSCAN structured light scanner. The non-human
161 sample came from museum collections and they came from different origins (i.e., wild-
162 shot, captivity and unknown origin). Their surface models were collected using
163 photogrammetry as described in Bucchi et al., (2020). Both scanned and
164 photogrammetry models are high resolution, therefore providing a good representation
165 of the original anatomy. The resolution of the models generated using surface scanner
166 and photogrammetry have been previously tested and found to be comparable
167 (Giacomini et al., 2019), thus allowing us to combine these data types in our analyses.
168 Only adult individuals were included in the study and right MC1s were preferred
169 (although left MC1s were reflected when their antimere was not present).

170

171 The fossil sample includes the right metacarpal from a *Homo neanderthalensis*, the
172 right metacarpal from a *Homo naledi* and the left metacarpal from an *Australopithecus*

173 *sediba*. The *H. neanderthalensis* sample was found in La Ferrassie archaeological site
174 in Savignac-de-Miremont, France. The skeleton was discovered in 1909 and is
175 estimated to be 70–50,000 years old (Guérin et al., 2015). The *Homo naledi* sample
176 (Morphosource identifier: S2110) was recovered in 2013 from the Rising Star cave
177 system in South Africa and has been dated to around 250,000 years ago (Dirks et al.,
178 2017). The *A. sediba* sample (Morphosource identifier: S2490) was taken from the
179 near complete wrist and hand of an adult female [Malapa Hominin 2 (MH2)] discovered
180 in Malapa, South Africa (Berger et al., 2010). The latter fossils were downloaded from
181 Morphosource <https://www.morphosource.org/>, whereas the Neanderthal was
182 obtained from a cast housed at the Catalan Institute of Human Paleoecology and
183 Social Evolution (IPHES).

184

185 2.2. 3DGM

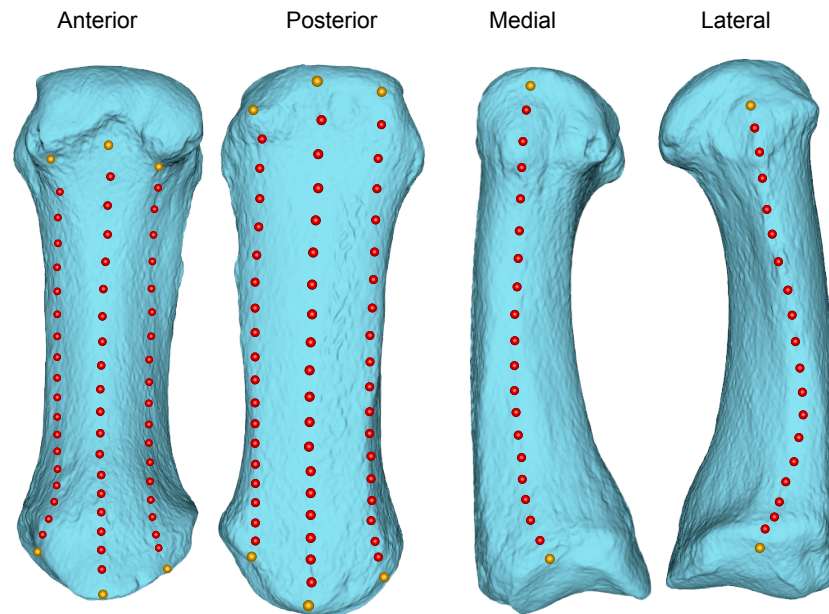
186 3D coordinates were collected using the software Landmark Editor 3.6 (Wiley et al.,
187 2005) to quantify the MC1's morphology. Eight curves comprising 20 equidistant
188 coordinates each were placed at pre-defined points on the MC1 (Figure 1). These
189 coordinates were chosen to provide a good representation of the overall shape of the
190 shaft of the bone. The first and last coordinates from each one of the eight curves were
191 treated as fixed landmarks, whereas all the rest of the coordinates (i.e., 144
192 coordinates) were considered as semi-landmarks. A generalized Procrustes
193 superimposition was performed on the coordinate data to remove differences due to
194 scale, translation, and rotation, thus obtaining shape variables (Bookstein, 1991). The
195 semi-landmarks were slid on the MC1's surface by minimizing bending energy
196 (Bookstein, 1997; Gunz, Mitteroecker, & Bookstein, 2005).

197

198 These obtained shape variables were then used in a principal component analysis
199 (PCA) to quantify overall shape variation. The data set of extant hominoids was then
200 grouped by genus and the Procrustes variance of observations in each group (i.e., the
201 mean squared Procrustes distance of each specimen from the mean shape of the
202 respective group) was computed as a simple measure to assess morphological
203 disparity within each one (Klingenberg & McIntyre, 1998; Zelditch, Sheets, & Fink,
204 2003). Procrustes variance was applied here as way to evaluate intra-genus variation,
205 and absolute differences in Procrustes variances were computed to test differences in
206 morphological disparity among groups (these differences statistically evaluated
207 through permutation). Then, a multi-group linear discriminant analysis (LDA) (also
208 known as canonical variate analysis) was run to maximize separation between groups
209 using the principal components (PCs) that accounted for 90% of the sample variance.
210 Performance was calculated using the confusion matrix from which the overall
211 classification accuracy was computed, as well as the Cohen's Kappa statistic
212 (Püschel, Marcé-Nogué, Gladman, et al., 2020; Püschel, Marcé-Nogué, Gladman,
213 Bobe, & Sellers, 2018). The complete dataset was resampled using a 'leave-one-
214 subject-out' cross-validation, as a way to asses classification performance (Kuhn &
215 Johnson, 2013). Pairwise PERMANOVA tests with Bonferroni corrections for multiple
216 comparisons were performed to assess for shape differences between the three
217 extant genera using the again PCs that accounted for 90% of the sample variance.
218 Euclidean distances were selected as similarity index.

219

220 All these analyses were carried out in R 3.5.1 (R Core Team, 2019), using the
221 'geomorph' 3.1.2 (Adams, Collyer, & Kaliontzopoulou, 2019) and 'MASS' 7.3-51.5
222 packages (Venables & Ripley, 2002).



223

224 Figure 1. Illustration of the 16 landmarks (black spheres) and 144 semi-landmarks (red spheres) used to quantify
225 MC1's body morphology.

226

227 **3 Results**

228 3.1 Principal component analysis

229 The PCA performed using the shape variables returned 102 PCs. The first 22 PCs
230 accounted for ~ 90% of the total variance of the sample, hence offering a reasonable
231 estimate of the total amount of MC1's shape variation, which were then used in the
232 LDA and pairwise PERMANOVA tests. The first three PCs in the PCA account for ~
233 57% of the total variance and display a relatively clear separation between the extant
234 African ape genera (Fig. 2a). PC1 explains 40.8 %, PC2 10.44% and PC3 5.43% of
235 total variance, respectively (Fig. 1a-d).

236

237 Violin plots of PC1 (Fig. 2b) show a notable difference between gorillas and humans
238 vs. chimpanzees. Humans and gorillas exhibit the highest PC1 scores, representing a
239 wider distal articular surface, a larger proximal articular surface, a significantly more

240 robust shaft. Chimpanzees show the lowest PC1 scores, representing a narrower
241 proximal articular surface, a smaller distal head, smaller radial and ulnar epicondyles
242 and a more gracile shaft. *H. neanderthalensis* falls within the human and gorilla
243 distributions and is distinct completely from the chimpanzees. *H. naledi* falls within the
244 human distribution, whilst *A. sediba* is characterized by a lower PC1 score and aligns
245 closer to the *Pan* distribution. None of the analyzed fossils fall within any of
246 interquartile ranges (IQR) (i.e., black bars in Fig. 1b-d) of any of the extant genera.

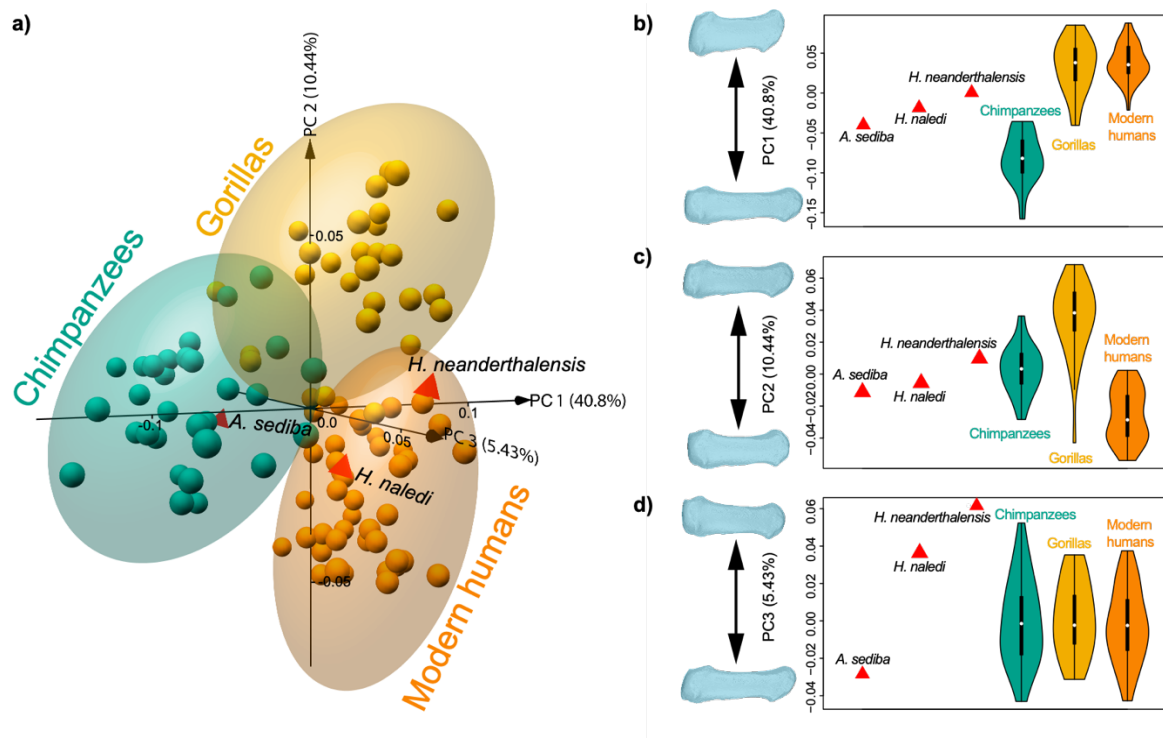
247

248 Violin plots of PC2 (Fig. 2c) shows distinct variation between the extant genera, with
249 a morphological continuum ranging from *Gorilla* (higher PC2 values), *Pan* (central PC2
250 values) and *H. sapiens* (lower PC2 scores). Interestingly, due to the presence of a
251 couple of outliers, the morphological variation in *Gorilla* encompasses the whole range
252 of observed morphological variation. The *Gorilla* sample has the highest PC2 scores,
253 representing an extended palmar lip, a more curved shaft and more rounded ends.
254 The modern human distribution shows the lowest PC2 scores, representing flatter
255 distal and proximal articular ends, as well as larger radial palmar condyles at the distal
256 end. The chimpanzee sample lies in between the gorilla and modern human samples
257 displaying an intermediate morphology. In a similar fashion as chimpanzees, the three
258 fossils are located at intermediate positions in PC2 distribution. *H. neanderthalensis*
259 and *H. naledi* display PC2 scores that are within the *Pan* IQR, whilst *A. sediba* has
260 lower values.

261

262 Violin plots of PC3 (Fig. 2d) show a similar distribution of PC scores for the three extant
263 genera. From a morphological perspective, higher scores are associated with more
264 robust morphologies displaying more marked muscular attachments (for the opponens

265 pollicis, first dorsal interosseous and abductor pollicis longus muscles), while lower
 266 values correspond to more gracile MC1s. *H. naledi* and *A. sediba* show values which
 267 are within the *Pan* or *H. sapiens* distribution, but outside their IQR and at opposite
 268 extremes of the axis. *H. neanderthalensis* lies outside the distribution of any of the
 269 extant genera, probably due to its particularly robust morphology and associated
 270 marked muscular insertion areas.



271
 272 Figure 2. Principal component analysis of the shape data: the a) three main axes of morphological variation are
 273 displayed (ellipses represent 95% confidence intervals, whilst fossils are shown as red tetrahedrons); Violin plots
 274 of the PCs scores of the analyzed sample are shown for b) PC1, c) PC2 and d) PC3 (fossil values are displayed
 275 as red triangles). The models closest to the mean shape was warped to match the multivariate mean using the thin
 276 plate spline method. The obtained average model was then warped to represent the variation along the three
 277 plotted PC axes (mag = 1).

278

279 3.2 Morphological disparity

280

281 To compare the amounts of shape variation between the extant genera, we used
282 Procrustes variance as a way to assess intra-genus variation. The obtained results
283 show that three extant genera show a similar magnitude of disparity. Nevertheless,
284 gorillas exhibit a higher Procrustes variance as compared to modern humans and
285 chimpanzees (Table 1a). Gorillas are significantly different to modern humans, and
286 chimpanzees when comparing absolute variance differences, whilst modern human
287 do not significantly differ from chimpanzees (Table 1b).
288

Table 1. Morphological disparity results

a) Procrustes variance			
Chimpanzees	0.004840776		
Gorillas	0.006378662		
Modern humans	0.004423507		
b) Pairwise differences			
	Chimpanzees	Gorillas	Modern humans
Chimpanzees		0.009	0.393
Gorillas	0.001537886		0.001
Modern humans	0.000417269	0.001955155	

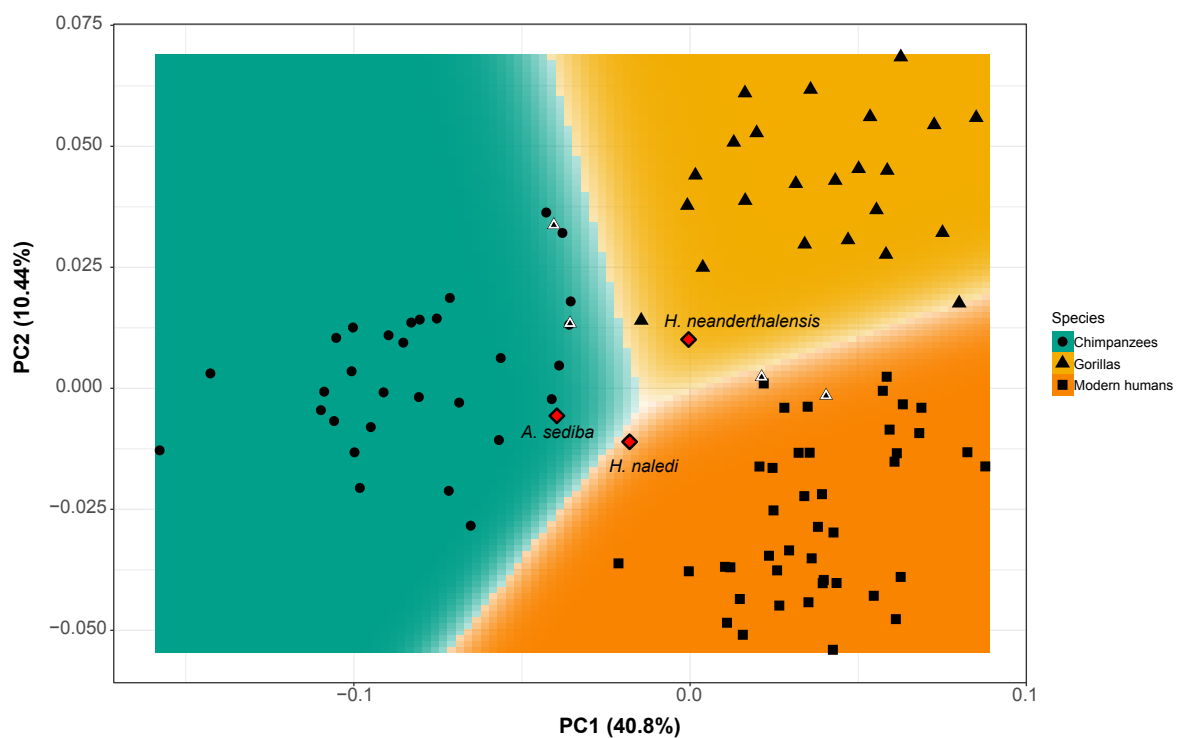
Above the diagonal: p-values (significant in bold); below the diagonal: absolute differences.

289

290 3.3 Linear discriminant analysis

291 The LDA model using the first 22 PCs clearly distinguishes between the three extant
292 genera, displaying an outstanding performance with almost perfect classification

293 results after cross-validation (Accuracy: 0.98; Cohen's Kappa: 0.97; Figure 3). When
294 using the obtained discriminant function to classify the fossils into the extant categories
295 (as way of assessing morphological affinities) (Table 2), the three of them were
296 robustly classified into the *Homo* category (all posterior probabilities were extremely
297 close to 1), hence indicating that, in spite of their differences, their morphology is closer
298 to that of modern humans. There were significant differences between all extant
299 genera when analyzing 22 PCs from the PCA carried out using the shape variables
300 (Table 3).



301
302 Figure 3. Decision boundary plot for the first 22 PCs the PCA carried out using the shape variables.
303 The two variables that contributed the most to each LDA models are displayed (i.e., PC1 and PC2).
304 The space is colored depending on what substrate preference the (LDA model predict that region
305 belongs to, whereas the lines between colored areas represent the decision boundaries. Color intensity
306 indicates the certainty of the prediction in a particular graph area (i.e., darker colors mean a higher
307 probability of belonging to a certain category). Symbols surrounded by a white rim correspond to
308 misclassified specimens for the plotted variables, whilst fossil are in red.
309

Table 2. Prediction results for the fossil sample.

	LDA model		
	Posterior probabilities		
Species	Chimpanzees	Gorillas	Modern humans
<i>Australopithecus sediba</i>	0.09	0.00	0.91
<i>Homo naledi</i>	0.00	0.00	1.00
<i>Homo neanderthalensis</i>	0.00	0.00	1.00

310

Table 3. Pairwise PERMANOVA results

	F-model	Bonferroni-corrected p-value
Modern humans vs. gorillas	15.84	0.0003
Modern humans vs. chimpanzees	68.87	0.0003
Chimpanzees vs. gorillas	42.03	0.0003

311

312 **4 Discussion**

313

314 The first hypothesis was that the shape of the human MC1 would differ significantly
315 from that of *Pan* and *Gorilla*, due to the variation in their manipulative capabilities and
316 locomotive behaviors. Results from the analyses provide strong support for this
317 hypothesis, confirming that there is indeed significant morphological variation between
318 the extant great apes. Interestingly, we also found clear differences between
319 chimpanzees and gorillas, with gorillas closer (i.e., more similar) to humans than to
320 chimpanzees (PC1). The second hypothesis was that all fossil hominin species would
321 exhibit an MC1 morphology more similar to humans than other great apes. The results
322 also support this hypothesis. However, it is important to notice that even though the

323 three fossils are more similar to the modern humans, they also display some distinct
324 features, different from those which would be typically expected in modern *H. sapiens*.

325

326 5.1 Humans and great apes MC1 shape

327 The 3DGM data indicate that modern human MC1 morphology is significantly different
328 from the rest of the extant hominids, therefore allowing us to accept the first
329 hypothesis. The human distal head is characterized by a flatter, larger distal articular
330 surface and larger radial and ulnar epicondyles. The proximal base of the human MC1
331 is also larger and flatter in both the radioulnar and dorsovolar aspects, with less
332 pronounced curvature than that seen in other hominid species. These are all
333 morphologies that are consistent with previous 3DGM analysis of the proximal (Marchi
334 et al., 2017) and distal (Galletta et al. 2019) surfaces of the human MC1. The shaft,
335 an area that has not previously been analyzed using 3DGM, is characterized by being
336 significantly more robust, with a greater curvature and a larger ridge on its lateral side,
337 corresponding to the insertion of the opponens pollicis muscle.

338

339 The flatter and larger distal articular surface in humans has been interpreted as an
340 adaptation that limits dorso-palmar motion whilst preventing radioulnar motion
341 (Barmakian, 1992), thereby stabilizing the MC1 and facilitating forceful power and
342 precision grasping. In apes that distal articular surface has a more pronounced
343 curvature, rendering the metacarpophalangeal joint (MCPJ) less stable and unable to
344 sustain high loads (Galletta et al., 2019). The pronounced radial and ulnar epicondyles
345 found at the distal head of the human MC1 (as described by PC1) serve a similar
346 purpose, reducing the range of motion and stabilizing the MCPJ. These epicondyles
347 act as anchor points for collateral ligaments, which insert at the base of the proximal

348 phalanx. When the thumb is flexed these ligaments tighten and limit the radioulnar
349 motion of the proximal phalanx (Imaeda et al., 1992). Larger epicondyles are therefore
350 thought to act as stronger anchors by providing a greater area for the collateral
351 ligaments to attach to, helping stabilize the MCPJ during the high forces that are
352 experienced by the thumb during manipulation (Galletta et al., 2019). The proximal
353 articular surface in humans is also flatter (as described by PC2), but in contrast this is
354 correlated with a higher range of motion at the trapeziometacarpal joint (TMCJ), rather
355 than a lower one (Marzke et al., 2010). It is this combination in humans of high mobility
356 at the TMCJ and low mobility at the MCPJ that facilitates a high level of manual
357 dexterity, whilst also allowing the thumb to sustain high loads during forceful tool use.
358 High mobility at the TMCJ plays a key role in the pad-to-pad opposition abilities of the
359 human hand, in which the thumb is able to rotate and touch the apical tip of each
360 phalanx. In many human manipulative activities like precision grips the thumb needs
361 to be highly abducted, which means that the load is radially shifted on the joint surface
362 (Lewis, 1977; Marchi et al., 2017). The observed larger radially extended proximal
363 surface is therefore important because, whilst it allows for a greater radial extension,
364 it also helps the joint resist high levels of radial displacement by providing a greater
365 surface area for the abducted MC1 (Hamrick, 1996).

366

367 We hypothesize that the morphological characteristics of the human MC1 shaft
368 presented here, such as a significantly more robust build, are likely adaptations that
369 further serve to facilitate forceful tool use. Indeed, a thicker MC1 shaft would be able
370 to better withstand the high levels of stress placed upon the thumb by sustained power
371 and precision grasping (Key & Dunmore, 2015; Marzke, Wullstein, & Viegas, 1992;
372 Rolian, Lieberman, & Zermeno, 2011). It has been also related to a greater

373 development of the thenar musculature attaching into the shaft that is highly active
374 during hard hammer percussion and that would favor thumb opposition (Marzke, 2013;
375 Marzke, Toth, Schick, & Reece, 1998).

376

377 5.1 Fossil hominin MC1 shape

378 The general scientific consensus in recent years is that *H. neanderthalensis* had a
379 hand morphology and manipulative capabilities that were very similar to those of
380 humans, challenging the previously held beliefs that *H. neanderthalensis* lacked the
381 derived adaptations for advanced and precise human-like tool use (Karakostis et al.,
382 2017; Karakostis, Hotz, Turloukis, & Harvati, 2018; Niewoehner, 2001, 2006; Tocheri
383 et al., 2008; Trinkaus & Villemeur, 1991). The results align well with this consensus,
384 with the *H. neanderthalensis* specimen showing several similarities with the modern
385 humans. The described morphology is one of a flatter (PC2) and larger (PC1) distal
386 articular surface, bigger epicondyles at the distal head (PC1) and a flatter proximal
387 articular surface (PC2). However, *H. neanderthalensis* also differs in exhibiting a
388 particularly robust MC1 with strongly marked muscular insertions.

389

390 Previous analysis on the thumb morphology of *Homo naledi* fossils has indicated that
391 it has derived characteristics compatible with forceful precision grip and human-like
392 manipulative abilities (Berger et al., 2015; Kivell, 2015). Such characteristics include
393 a well-developed crest for the opponens pollicis insertion and flat distal/proximal
394 articular surfaces (Kivell et al., 2015; Galletta et al. 2019). The results generally agree
395 with these observations and conclusions, whilst also presenting some potentially new
396 insights. The morphology of the *H. naledi* sample had a human-like robustness of the
397 shaft (PC1), suggesting that the MC1 was adapted to sustain high loads, such as those

398 experienced during forceful tool use. This suggests that *H. naledi* was potentially
399 capable of a degree of advanced manipulation, such as forceful precision and power
400 grasping. These findings are therefore consistent with previous functional
401 interpretations of *H. naledi* thumb morphology (Galletta et al. 2019). Whilst the
402 evidence suggests that *H. naledi* was almost certainly able to perform an certain
403 degree of advanced manipulation, and was likely a tool-user, it also suggests that it
404 had not yet showed the full repertoire of manipulative adaptations exhibited by humans
405 and *H. neanderthalensis* (Berger et al., 2015; Kivell et al., 2015; Galletta et al., 2019).
406

407 Previous analysis of *A. sediba* hand morphology has found that it possessed a number
408 of advanced *Homo*-like features, such as a longer thumb relative to shorter fingers,
409 that potentially indicate advanced manipulative capabilities, while retaining primitive
410 traits as a gracile MC1, similar to those of other australopithecines (Kivell et al., 2011).
411 Recent 3DGM studies that have analyzed the MC1 in particular have come to the
412 conclusion that if *A. sediba* was indeed utilizing tools, as some hand proportion and
413 trabecular evidence suggests (Kivell et al., 2011; Skinner et al., 2015), then it was
414 doing so in a way that differed from that of early *Homo* and modern humans (Marchi
415 et al., 2017; Galletta et al., 2019). This conclusion was reached due to aspects of their
416 MC1 morphology that were deemed inconsistent with the ability to employ forceful
417 precision grips, namely a gracile MC1 shaft, more curved proximal articular surface
418 and smaller radial and ulnar epicondyles. These morphologies suggest that the range
419 of motion would not have been great enough at the TMCJ to facilitate the necessary
420 abduction-adduction for thumb opposition and pad-pad precision grips. The results
421 agree with this consensus, with the *A. sediba* sample presenting a gracile shaft (PC1),
422 and smaller epicondyles at the distal head. These morphologies suggest that the *A.*

423 *sediba* MC1 did not have the strength or stability to withstand the forces involved with
424 precision grips, nor the range of motion at the TMCJ to facilitate them. Overall the
425 results therefore align with previous research, in the sense that they present *A. sediba*
426 as having a patchwork of primitive and derived characteristics, a few of which are
427 indicators of an ability to use tools, but most of which suggest that this ability was
428 incipient and certainly not comparable to the forceful precision grip abilities of humans
429 and *H. neanderthalensis*.

430

431 **6. Conclusion**

432

433 The aim of this study was to quantify the 3D morphology of the first metacarpal in
434 extant African hominoids, in order to facilitate a more informed functional interpretation
435 of fossil hominin morphology. The results are in general agreement with previous
436 studies on the morphology of the MC1 in extant and extinct hominids and the
437 inferences made by them. This study found that the human MC1 is characterized by
438 a distinct suite of traits, not present to the same extent in non-human great apes, that
439 are consistent with an ability to use forceful precision and power grips; namely flatter
440 proximal and distal ends, larger epicondyles at the distal head and a more robust shaft.
441 This morphology was also found to align very closely with that of the *H.*
442 *neanderthalensis* sample, supporting all the evidence that indicates that Neanderthals
443 were functionally capable of utilizing tools in the same way as modern humans.
444 Analysis of the *H. naledi* specimen suggested that it had a number of human-like
445 adaptations consistent with an ability to employ advanced manipulation and was
446 therefore likely able to use stone tools in a similar way to humans. The *A. sediba* fossil
447 presented a number of derived MC1 features that indicate a degree of dexterity, but

448 also several traits which were more similar to the African apes (i.e., probably primitive
449 traits). Overall the results obtained both aligned with and added to past functional
450 interpretations of hominin morphology, thereby reinforcing the validity of 3DGM as a
451 method of quantifying MC1 morphology and providing a deeper insight into the
452 function and structure of the thumb in both extant hominids and fossil hominins.

453

454 **Acknowledgments**

455 We are grateful to the following curators and institutions for the access of the ape
456 specimens: Emmanuel Gilissen (AfricaMuseum), Anneke H. van Heteren and Michael
457 Hiermeier (Zoologische Staatssammlung München), Javier Quesada (Museu de
458 Ciències Naturals de Barcelona), José Miguel Carretero (Universidad de Burgos). AB
459 was partially funded by a Becas Chile scholarship, whilst TP was funded by the
460 Leverhulme Trust Early Career Fellowship, ECF-2018-264. This study was funded by
461 the research projects AGAUR 2017 SGR 1040 and MICINN-FEDER PGC2018-
462 093925-B-C32.

463

464 **Author contributions**

465 TAP and AB designed the study. AB and CL generated the 3D models. JM and TAP
466 analyzed the data. TAP carried out the data visualizations. All authors interpreted the
467 data and wrote the manuscript.

468

469 **ORCID**

470 Thomas A. Püschel <https://orcid.org/0000-0002-2231-2297>

471 Ana Bucchi <https://orcid.org/0000-0002-1247-230X>

472 Carlos Lorenzo <https://orcid.org/0000-0001-5706-293X>

473 **References**

474

475 Adams, D. C., Collyer, M. L., & Kaliontzopoulou, A. (2019). *Geomorph: Software for*
476 *geometric morphometric analysis. R package version 3.1.0.*

477 Alba, D. M., Moyà-Solà, S., & Köhler, M. (2003). Morphological affinities of the
478 *Australopithecus afarensis* hand on the basis of manual proportions and relative
479 thumb length. *Journal of Human Evolution*, 44(2), 225–254.
480 [https://doi.org/10.1016/S0047-2484\(02\)00207-5](https://doi.org/10.1016/S0047-2484(02)00207-5)

481 Almécija, S., & Alba, D. M. (2014). On manual proportions and pad-to-pad precision
482 grasping in *Australopithecus afarensis*. *Journal of Human Evolution*, 73, 88–92.
483 <https://doi.org/10.1016/j.jhevol.2014.02.006>

484 Almécija, S., Moyà-Solà, S., & Alba, D. M. (2010). Early origin for human-like precision
485 grasping: A comparative study of pollical distal phalanges in fossil hominins. *PLOS*
486 *ONE*, 5(7), e11727. <https://doi.org/10.1371/journal.pone.0011727>

487 Almécija, S., Smaers, J. B., & Jungers, W. L. (2015). The evolution of human and ape hand
488 proportions. *Nature Communications*, 6, 1–11. <https://doi.org/10.1038/ncomms8717>

489 Aubriot, J. H., & Tubiana, R. (1981). The metacarpophalangeal joint of the thumb. *The Hand*,
490 1, 184–187.

491 Barmakian, J. T. (1992). Anatomy of the joints of the thumb. *Hand Clinics*, 8(4), 683–691.

492 Berger, L. R., Hawks, J., de Ruiter, D. J., Churchill, S. E., Schmid, P., Delezene, L. K., ...
493 Zipfel, B. (2015). *Homo naledi*, a new species of the genus *Homo* from the Dinaledi
494 Chamber, South Africa. *ELife*, 4(September2015), 1–35.
495 <https://doi.org/10.7554/eLife.09560>

496 Berger, L. R., Ruiter, D. J. de, Churchill, S. E., Schmid, P., Carlson, K. J., Dirks, P. H. G. M.,
497 & Kibii, J. M. (2010). *Australopithecus sediba*: A new species of Homo-like

- 498 australopith from South Africa. *Science*, 328(5975), 195–204.
- 499 <https://doi.org/10.1126/science.1184944>
- 500 Boesch, C., & Boesch, H. (1990). Tool use and tool making in wild chimpanzees. *Folia*
501 *Primatologica*, 54(1–2), 86–99.
- 502 Bookstein, F. L. (1991). *Morphometric Tools for Landmark Data: Geometry and Biology*.
503 Cambridge: Cambridge University Press.
- 504 Bookstein, F. L. (1997). Landmark methods for forms without landmarks: morphometrics of
505 group differences in outline shape. *Medical Image Analysis*, 1(3), 225–243.
506 [https://doi.org/10.1016/S1361-8415\(97\)85012-8](https://doi.org/10.1016/S1361-8415(97)85012-8)
- 507 Breuer, T., Ndoundou-Hockemba, M., & Fishlock, V. (2005). First observation of tool use in
508 wild gorillas. *PLoS Biology*, 3(11), e380.
- 509 Bucchi, A., Luengo, J., Fuentes, R., Arellano-Villalón, M., Lorenzo, C. (2020).
510 Recommendations for improving photo quality in close range photogrammetry,
511 exemplified in hand bones of chimpanzees and gorillas. *International Journal of*
512 *Morphology*, 38(2), 348–355. <https://doi.org/10.4067/S0717-95022020000200348>
- 513 Casillas Garcia, J. A., & Alvarez, G. A. (2005). *La Actuacion Arqueologica en el “Solar de*
514 *Caballeria” y el Convento de San Pablo de Burgos*. Burgos: Ayuntamiento de
515 Burgos, Instituto Municipal de Cultura.
- 516 Dirks, P. H., Roberts, E. M., Hilbert-Wolf, H., Kramers, J. D., Hawks, J., Dosseto, A., ...
517 Berger, L. R. (2017). The age of homo naledi and associated sediments in the rising
518 star cave, South Africa. *ELife*, 6. <https://doi.org/10.7554/eLife.24231>
- 519 Feix, T., Kivell, T. L., Pouydebat, E., & Dollar, A. M. (2015). Estimating thumb-index finger
520 precision grip and manipulation potential in extant and fossil primates. *Journal of the*
521 *Royal Society, Interface*, 12(106), 20150176–. <https://doi.org/10.1098/rsif.2015.0176>

- 522 Galletta, L., Stephens, N. B., Bardo, A., Kivell, T. L., & Marchi, D. (2019). Three-
523 dimensional geometric morphometric analysis of the first metacarpal distal articular
524 surface in humans, great apes and fossil hominins. *Journal of Human Evolution*, *132*,
525 119–136. <https://doi.org/10.1016/j.jhevol.2019.04.008>
- 526 Giacomini, G., Scaravelli, D., Herrel, A., Veneziano, A., Russo, D., Brown, R. P., & Meloro,
527 C. (2019). 3D photogrammetry of bat skulls: Perspectives for macro-evolutionary
528 analyses. *Evolutionary Biology*, *46*, 249–259. [https://doi.org/10.1007/s11692-019-](https://doi.org/10.1007/s11692-019-09478-6)
529 [09478-6](https://doi.org/10.1007/s11692-019-09478-6)
- 530 Gommery, D., & Senut, B. (2006). La phalange distale du pouce d’Orrorin tugenensis
531 (Miocene supérieur du Kenya). *Geobios*, *39*(3), 372–384.
- 532 Green, D. J., & Gordon, A. D. (2008). Metacarpal proportions in *Australopithecus africanus*.
533 *Journal of Human Evolution*, *54*(5), 705–719.
534 <https://doi.org/10.1016/j.jhevol.2007.10.007>
- 535 Guérin, G., Frouin, M., Talamo, S., Aldeias, V., Bruxelles, L., Chiotti, L., ... Jain, M. (2015).
536 A multi-method luminescence dating of the Palaeolithic sequence of La Ferrassie
537 based on new excavations adjacent to the La Ferrassie 1 and 2 skeletons. *Journal of*
538 *Archaeological Science*, *58*, 147–166.
- 539 Gunz, P., Mitteroecker, P., & Bookstein, F. L. (2005). Semilandmarks in three dimensions. In
540 D.E. Slice (Ed.), *Modern morphometrics in physical anthropology* (pp. 73–98).
541 Boston, MA: Springer US.
- 542 Hamrick, M. W. (1996). Articular size and curvature as determinants of carpal joint mobility
543 and stability in strepsirhine primates. *Journal of Morphology*, *230*(2), 113–127.
- 544 Holliday, T. W., Churchill, S. E., Carlson, K. J., DeSilva, J. M., Schmid, P., Walker, C. S., &
545 Berger, L. R. (2018). Body size and proportions of *Australopithecus sediba*.
546 *PaleoAnthropology*, (January), 406–422. <https://doi.org/10.4207/PA.2018.ART118>

- 547 Imaeda, T., An, K. N., & Cooney 3rd, W. P. (1992). Functional anatomy and biomechanics
548 of the thumb. *Hand Clinics*, 8(1), 9–15.
- 549 Karakostis, F. A., Hotz, G., Scherf, H., Wahl, J., & Harvati, K. (2017). Occupational manual
550 activity is reflected on the patterns among hand entheses. *American Journal of*
551 *Physical Anthropology*, 164(1), 30–40. <https://doi.org/10.1002/ajpa.23253>
- 552 Karakostis, F. A., Hotz, G., Tournloukis, V., & Harvati, K. (2018). Evidence for precision
553 grasping in Neandertal daily activities. *Science Advances*, 4(9), eaat2369.
554 <https://doi.org/10.1126/sciadv.aat2369>
- 555 Key, A. J. (2016). Manual loading distribution during carrying behaviors: Implications for
556 the evolution of the hominin hand. *PloS One*, 11(10), e0163801.
- 557 Key, A. J. M., & Dunmore, C. J. (2015). The evolution of the hominin thumb and the
558 influence exerted by the non-dominant hand during stone tool production. *Journal of*
559 *Human Evolution*, 78, 60–69. <https://doi.org/10.1016/j.jhevol.2014.08.006>
- 560 Kivell, T. L., Kibii, J. M., Churchill, S. E., Schmid, P., & Berger, L. R. (2011).
561 Australopithecus sediba Hand Demonstrates Mosaic Evolution of Locomotor and
562 Manipulative Abilities. *Science*, 333(6048), 1411–1417.
563 <https://doi.org/10.1126/science.1202625>
- 564 Kivell, T.L. (2015). Evidence in Hand: recent discoveries and the early evolution of human
565 manual manipulation. *Philosophical Transactions of the Royal Society*, 370.
- 566 Klingenberg, C. P., & McIntyre, G. S. (1998). Geometric morphometrics of developmental
567 instability: Analyzing patterns of fluctuating asymmetry with Procrustes methods.
568 *Evolution*, 52(5), 1363–1375. <https://doi.org/10.2307/2411306>
- 569 Kuhn, M., & Johnson, K. (2013). *Applied Predictive Modeling*. New York: Springer.
570 https://doi.org/10.1007/978-1-4614-6849-3_11

- 571 Lewis, O. J. (1977). Joint remodelling and the evolution of the human hand. *Journal of*
572 *Anatomy*.
- 573 Marchi, D., Proctor, D. J., Huston, E., Nicholas, C. L., & Fischer, F. (2017). Morphological
574 correlates of the first metacarpal proximal articular surface with manipulative
575 capabilities in apes, humans and South African early hominins. *Comptes Rendus*
576 *Palevol*, 16(5), 645–654. <https://doi.org/10.1016/j.crpv.2016.09.002>
- 577 Marzke, M. W. (2013). Tool making, hand morphology and fossil hominins. *Philosophical*
578 *Transactions of the Royal Society B: Biological Sciences*, 368(1630), 20120414.
579 <https://doi.org/10.1098/rstb.2012.0414>
- 580 Marzke, M. W., & Marzke, R. F. (2000). Evolution of the human hand: approaches to
581 acquiring, analysing and interpreting the anatomical evidence. *The Journal of*
582 *Anatomy*, 197(1), 121–140.
- 583 Marzke, M. W., Tocheri, M. W., Steinberg, B., Femiani, J. D., Reece, S. P., Linscheid, R. L.,
584 ... Marzke, R. F. (2010). Comparative 3D quantitative analyses of trapeziometacarpal
585 joint surface curvatures among living catarrhines and fossil hominins. *American*
586 *Journal of Physical Anthropology*, 141(1), 38–51. <https://doi.org/10.1002/ajpa.21112>
- 587 Marzke, M. W., Wullstein, K. L., & Viegas, S. F. (1992). Evolution of the power (“squeeze”)
588 grip and its morphological correlates in hominids. *American Journal of Physical*
589 *Anthropology*, 89(3), 283–298. <https://doi.org/10.1002/ajpa.1330890303>
- 590 Marzke, M. W., Marchant, L. F., McGrew, W. C., & Reece, S. P. (2015). Grips and hand
591 movements of chimpanzees during feeding in Mahale Mountains National Park,
592 Tanzania. *American Journal of Physical Anthropology*, 156(3), 317–326.
- 593 Marzke, M. W., Toth, N., Schick, K., & Reece, S. (1998). EMG Study of Hand Muscle
594 Recruitment During Hard Hammer Percussion Manufacture of Oldowan Tools.
595 *American Journal of Physical Anthropology*, 105(3), 315–32.

- 596 Marzke, M. W., & Wullstein, K. L. (1996). Chimpanzee and human grips: A new
597 classification with a focus on evolutionary morphology. *International Journal of*
598 *Primatology*, 17(1), 117–139. <https://doi.org/10.1007/BF02696162>
- 599 Napier, J. R. (1955). The form and function of the carpo-metacarpal joint of the thumb.
600 *Journal of Anatomy*, 89(3), 362–369.
- 601 Napier, J. R. (1956). The prehensile movements of the human hand. *The Journal of Bone and*
602 *Joint Surgery. British Volume*, 38(4), 902–913.
- 603 Napier, J. R. (1960). Studies of the hands of living primates. *Proceedings of the Zoological*
604 *Society of London*, 134(4), 647–657.
- 605 Niewoehner, W. A. (2001). Behavioral inferences from the Skhul/Qafzeh early modern
606 human hand remains. *Proceedings of the National Academy of Sciences*, 98(6), 2979–
607 2984. <https://doi.org/10.1073/pnas.041588898>
- 608 Niewoehner, W. A. (2006). Neanderthal hands in their proper perspective. In J-J. Hublian, K.
609 Harvati & T. Harrison (Eds.), *Neanderthals revisited: New approaches and*
610 *perspectives* (pp. 157–190). Dordrecht: Springer.
- 611 Püschel, T. A., Marcé-Nogué, J., Chamberlain, A. T., Yoxall, A., & Sellers, W. I. (2020). The
612 biomechanical importance of the scaphoid-centrale fusion during simulated knuckle-
613 walking and its implications for human locomotor evolution. *Scientific Reports*, 10(1),
614 1–7. <https://doi.org/10.1038/s41598-020-60590-6>
- 615 Püschel, T. A., Marcé-Nogué, J., Gladman, J., Patel, B. A., Almécija, S., & Sellers, W. I.
616 (2020). Getting its feet on the ground: Elucidating Paralouatta’s semi-terrestriality
617 using the virtual morpho-functional toolbox. *Frontiers in Earth Science*, 8, 79.
618 <https://doi.org/10.3389/feart.2020.00079>
- 619 Püschel, T. A., Marcé-Nogué, J., Gladman, J. T., Bobe, R., & Sellers, W. I. (2018). Inferring
620 locomotor behaviours in Miocene New World monkeys using finite element analysis,

- 621 geometric morphometrics and machine-learning classification techniques applied to
622 talar morphology. *Journal of The Royal Society Interface*, 15(146), 20180520.
623 <https://doi.org/10.1098/rsif.2018.0520>
- 624 R Core Team. (2019). *R: A language and environment for statistical computing*. R
625 Foundation for Statistical Computing, Vienna, Austria. URL [http://www.R-](http://www.R-project.org/)
626 [project.org/](http://www.R-project.org/).
- 627 Richmond, B. G., & Strait, D. S. (2000). Evidence that humans evolved from a knuckle-
628 walking ancestor. *Nature*, 404(6776), 382–385. <https://doi.org/10.1038/35006045>
- 629 Rightmire, G. P. (1972). Analysis Metacarpal Swartkrans. *Science*, 176, 159–161.
- 630 Rolian, C., Lieberman, D. E., & Zermeno, J. P. (2011). Hand biomechanics during simulated
631 stone tool use. *Journal of Human Evolution*, 61(1), 26–41.
632 <https://doi.org/10.1016/j.jhevol.2011.01.008>
- 633 Sanz, C., Call, J., & Morgan, D. (2009). Design complexity in termite-fishing tools of
634 chimpanzees (*Pan troglodytes*). *Biology Letters*, 5(3), 293–296.
- 635 Sanz, C. M., & Morgan, D. B. (2007). Chimpanzee tool technology in the Goualougo
636 Triangle, Republic of Congo. *Journal of Human Evolution*, 52(4), 420–433.
- 637 Skinner, M. M., Stephens, N. B., Tsegai, Z. J., Foote, A. C., Nguyen, N. H., Gross, T., ...
638 Kivell, T. L. (2015). Human-like hand use in *Australopithecus africanus*. *Science*,
639 347(6220), 395–399. <https://doi.org/10.1126/science.1261735>
- 640 Susman, R. L. (1998). Hand function and tool behavior in early hominids. *Journal of Human*
641 *Evolution*, 35(1), 23–46. <https://doi.org/10.1006/jhev.1998.0220>
- 642 Tocheri, M. W., Orr, C. M., Jacofsky, M. C., & Marzke, M. W. (2008). The evolutionary
643 history of the hominin hand since the last common ancestor of *Pan* and *Homo*.
644 *Journal of Anatomy*, 212(4), 544–562. [https://doi.org/10.1111/j.1469-](https://doi.org/10.1111/j.1469-7580.2008.00865.x)
645 7580.2008.00865.x

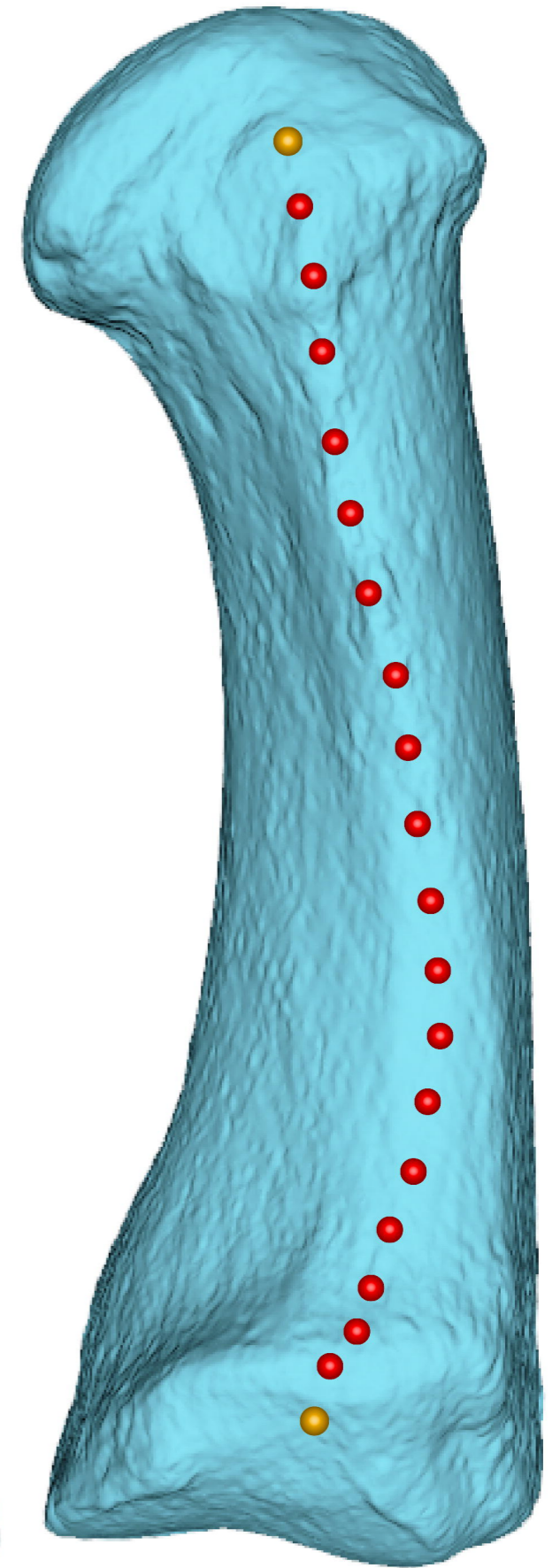
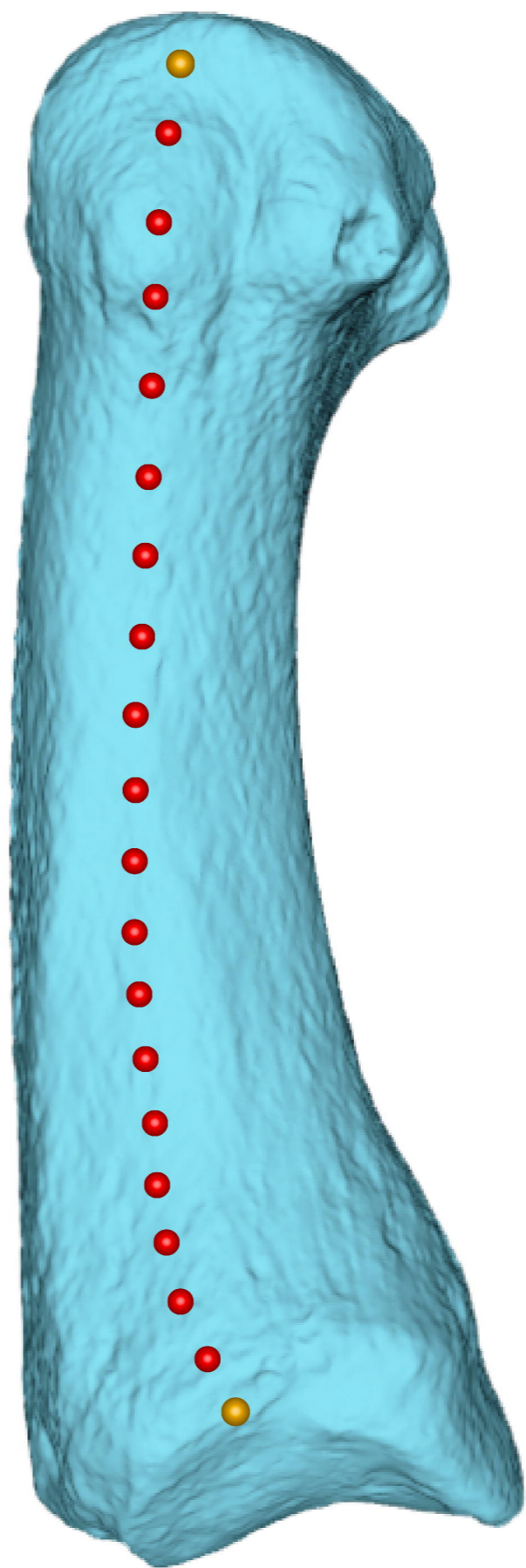
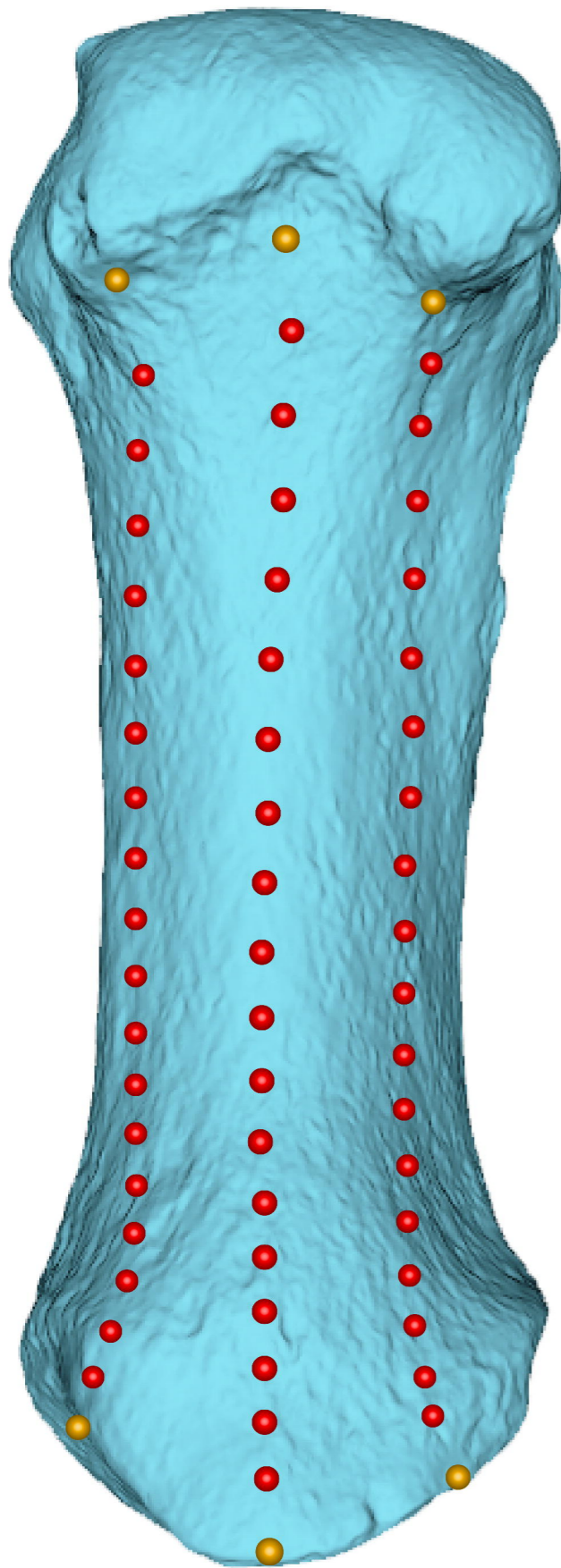
- 646 Trinkaus, E., & Villemeur, I. (1991). Mechanical advantages of the Neandertal thumb in
647 flexion: A test of an hypothesis. *American Journal of Physical Anthropology*, 84(3),
648 249–260. <https://doi.org/10.1002/ajpa.1330840303>
- 649 Tuttle, R. H. (1969). Quantitative and functional studies on the hands of the Anthroidea. I.
650 The Hominoidea. *Journal of Morphology*, 128(3), 309–363.
- 651 Venables, W. N., & Ripley, B. D. (2002). *Modern Applied Statistics with S* (4th ed.). New
652 York: Springer-Verlag.
- 653 Wiley, D. F., Amenta, N., Alcantara, D. A., Ghost, D., Kil, Y. J., Delson, E., ... Hamann, B.
654 (2005). Evolutionary morphing. *EEE Visualization, 2005. VIS 05*.
- 655 Zelditch, M. L., Sheets, H. D., & Fink, W. L. (2003). The ontogenetic dynamics of shape
656 disparity. *Paleobiology*, 29(1), 139–156.
- 657

Anterior

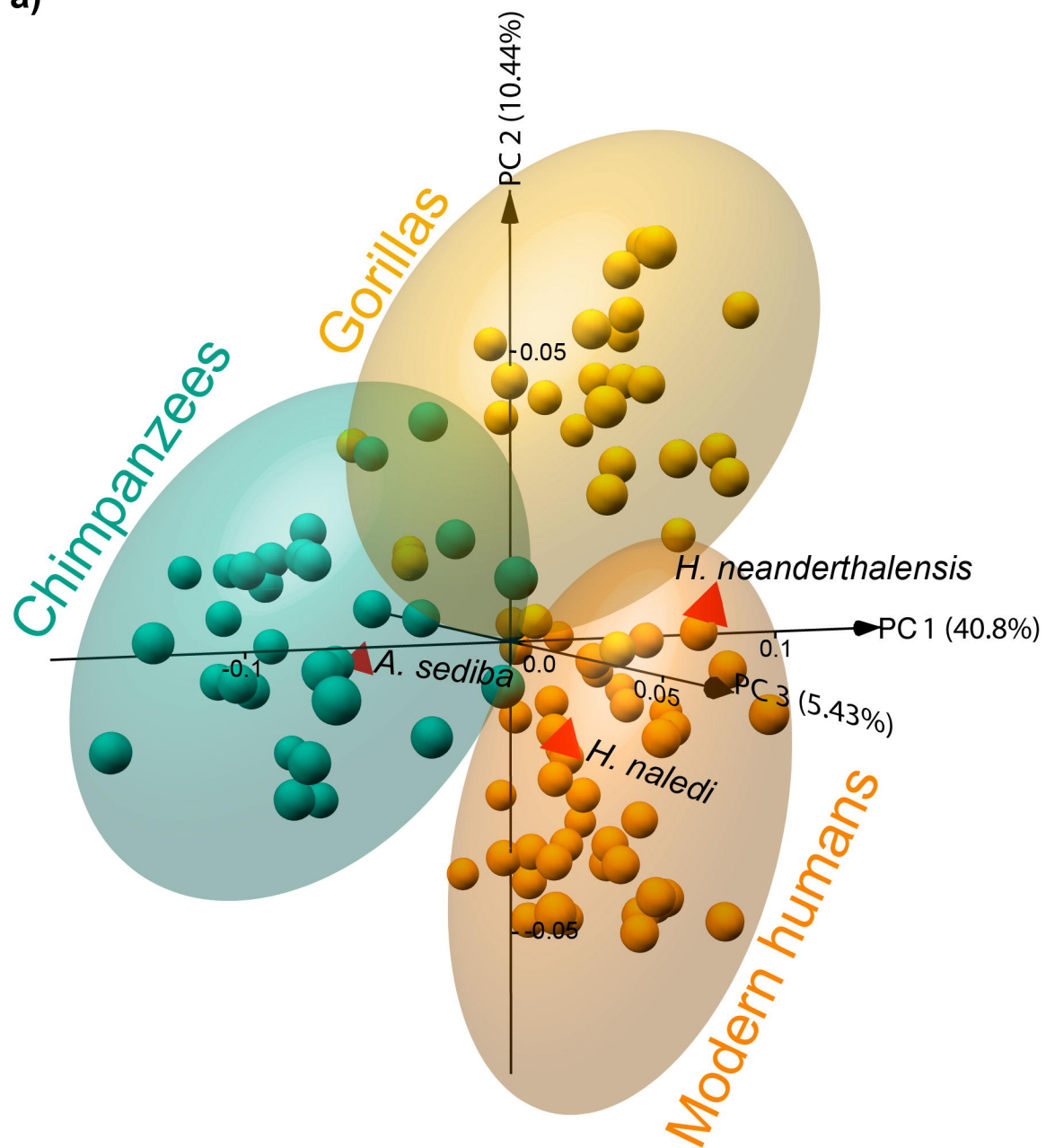
Posterior

Medial

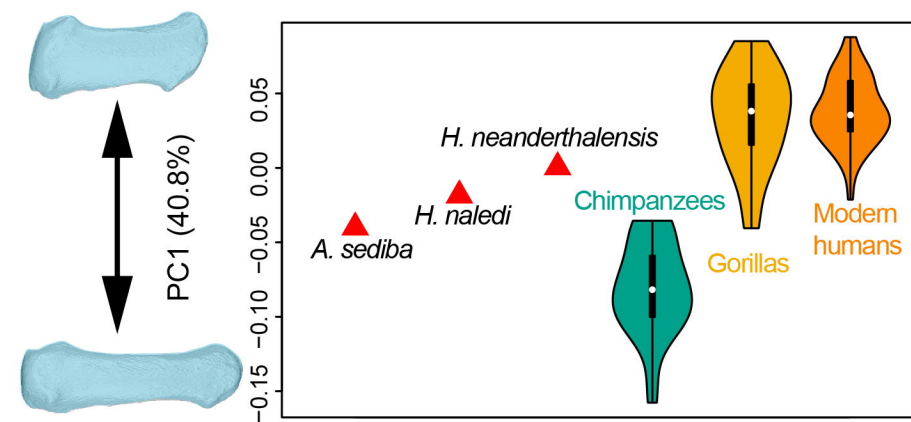
Lateral



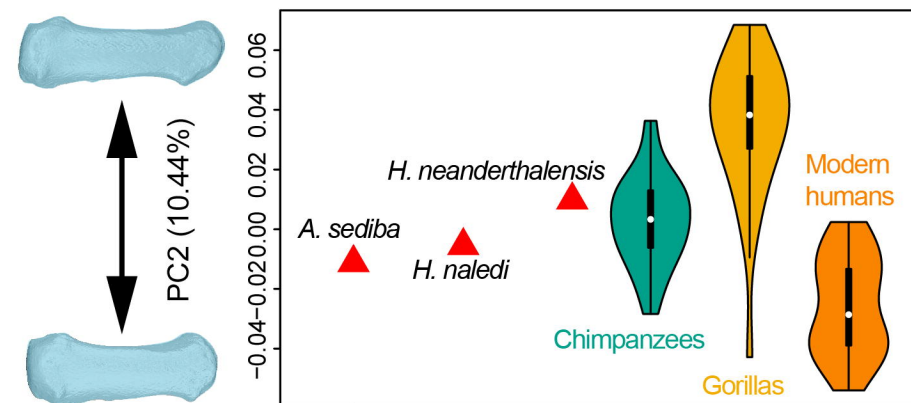
a)



b)



c)



d)

